Spectral Imaging With Dual-layer Spectral Detector Computed Tomography for Acute Coronary Syndrome

Junji Mochizuki
Minamino Cardiovascular Hospital
Takeshi Nakaura (kff00712@nifty.com)
Department of Diagnostic Radiology, Graduate School of Medical Sciences, Kumamoto University
https://orcid.org/0000-0002-9010-0341
Naofumi Yoshida
Department of Diagnostic Radiology, Graduate School of Medical Sciences, Kumamoto University
Yasunori Nagayama
Department of Diagnostic Radiology, Graduate School of Medical Sciences, Kumamoto University
Masafumi Kidoh
Department of Diagnostic Radiology, Graduate School of Medical Sciences, Kumamoto University
Hiroyuki Uetani
Department of Diagnostic Radiology, Graduate School of Medical Sciences, Kumamoto University
Yoshinori Funama
Department of Medical Physics, Faculty of Life Sciences, Kumamoto University
Yoshiki Hata
Minamino Cardiovascular Hospital
Minako Azuma
Department of Medical Physics, Faculty of Life Sciences, Kumamoto University
Toshinori Hirai
Department of Diagnostic Radiology, Graduate School of Medical Sciences, Kumamoto University

Research Article

Keywords: Dual-Energy Scanned Projection, Multidetector Computed Tomography, Acute Coronary Syndrome, Myocardial Perfusion

Posted Date: May 25th, 2021

DOI: https://doi.org/10.21203/rs.3.rs-544935/v1

Abstract

Purpose: To evaluate the feasibility of spectral imaging with dual-layer spectral detector computed tomography (CT) for the diagnosis of acute coronary syndrome.

Methods: We identified 33 consecutive patients who underwent cardiac CT using dual-layer spectral detector CT and were diagnosed with acute ischemic syndrome by an invasive coronary angiography. We reconstructed 120 kVp images and generated virtual monochromatic images (VMIs; 40–200 keV in 10 keV increments), iodine concentration maps, and effective atomic number (Z) maps. We calculated the contrast and contrast-to-noise noise ratio (CNR) between myocardial normal and hypo-perfusion and chose the VMIs with the best CNR for quantitative analysis. We compared the image noise, contrast, and CNR of 120 kVp images and the best VMIs, CT value, iodine concentration, and effective Z between myocardial normal and hypo-perfusion with the paired t-test.

Results: As the X-ray energy decreased, venous attenuation, contrast, and CNR gradually increased. The 40 keV image yielded the best CNR. There was no significant difference in image noise between the 120 kVp and 40 keV images. The contrast and CNR between myocardial normal and hypo-perfusion were significantly higher in 40 keV images than those in 120 kVp images. The iodine concentration and the effective Z were significantly higher in normal myocardium than those in hypo-perfused myocardium.

Conclusion: Spectral imaging with dual-layer spectral detector CT is a feasible technique to detect the hypo-perfused area of acute ischemic syndrome.

Introduction

Coronary thrombosis is generally accepted as the direct cause of acute coronary syndrome (ACS), and most coronary thrombi occur due to rupture or fistulation of the coronary plaque [1, 2]. Many studies have suggested that coronary computed tomography (CT) angiography has a high sensitivity and negative predictive value for significant coronary stenosis [3]. However, previous reports have also suggested that the percentage of coronary stenosis only modestly correlates with decreased myocardial blood flow [4]. Additionally, serial coronary angiography demonstrated that plaque rupture often occurs at sites with less severe stenosis [5, 6]. Therefore, coronary stenosis detected by coronary CT angiography might be inadequate to diagnose the culprit vessel for ACS, as many coronary arteries with intermediate stenosis (50–70%) can undergo unnecessary additional testing and treatments. A previous study suggested that rest CT perfusion by routine cardiac CT scan can increase the positive predictive value of ACS; however, the sensitivity of this method is only 33 % (3/9 patients) [7].

Dual-energy CT (DECT) can create virtual monochromatic images (VMIs) at different monochromatic X-ray energies (keV) based on the two different energy datasets. The reported advantages of VMIs include reducing beam-hardening artifacts and providing more accurate quantitative attenuation measurements [8, 9]. VMIs at low keV can increase contrast enhancement compared with the conventional tube technique [10]. However, no studies have reported the usefulness of rest cardiac DECT for ACS. Recently,

dual-layer DECT (DL-DECT) has been introduced for clinical use [11–13]. DL-DECT can overcome the disadvantage of increased image noise at low-energy levels. A previous study reported that VMIs at lower energy levels increased image quality of myocardial late iodine enhancement [14]; however, to the best of our knowledge, no previous study has compared VMIs obtained with DL-DECT with the images obtained with a conventional 120 kVp protocol to evaluate ACS.

The purpose of this study was to evaluate the feasibility of spectral imaging with dual-layer spectral detector CT for the diagnosis of ACS.

Methods

This retrospective study received institutional review board approval; the requirement for written informed consent was waived.

Study population

This was a retrospective study of the clinical records of ACS patients who underwent cardiac CT at our institution between January 2017 and March 2018. In this study period, coronary CT angiography was performed on 3177 patients with suspected or confirmed coronary artery disease for clinical reasons, based on the guidance of the American College of Cardiology [15]. Among these patients, 46 patients were diagnosed with ACS by invasive coronary angiography, of which 13 patients were excluded because of different CT protocols (n=9) or poor image quality (n=4). The remaining 33 patients were enrolled in this study and included 22 men and 11 women with a mean age of 62 years (range: 42–91 years) and a mean body weight of 60.3 kg (range: 32–99 kg).

Cardiac CT image acquisition

All patients were scanned with a dual-layer spectral detector CT scanner (iQon Spectral CT; Philips Healthcare, Best, the Netherlands). Individuals presenting with a baseline heart rate of >65 beats/min received an oral β-blocker (10–20 mg Inderal; AstraZeneca, Osaka, Japan) 60 min before the scan. Standard coronary CT angiography was performed with a 13 s intravenous infusion of Iopamiron 370 (240 mgI/mL; Bayer HealthCare, Osaka, Japan). The acquisition parameters for cardiac CT imaging were as follows (Table 1): detector collimation, 64 × 0.625 mm; tube rotation time, 270 ms; tube voltage, 120 kVp; tube current, 228.6 ± 57.5 mA (range, 100–370 mA); and volume CT dose index, 22.2 ± 5.5 mGy (range, 4.9–34.5 mGy).

CT Image Reconstruction

The spectral-based image data were post-processed at a workstation (Spectral Diagnostic Suite; Philips Healthcare) to generate VMIs at 17 different energy levels (40–200 keV) with a spectral level of 3 (manufacturer's recommendation). We used conventional CT images reconstructed with IR (iDose level 3; Philips Healthcare) as controls. We also reconstructed the quantitative, iodine density, and effective atomic number images. The slice thickness of all CT images was 1 mm.

Quantitative image analysis

A radiology technologist with 15 years of experience with cardiac CT performed the quantitative analysis of the axial images. CT attenuation of normal myocardium (HU_{normal}) and hypo-perfused myocardium (HU_{hypo}) was measured by placing circular region of interests in axial cardiac CT images. Normal and hypo-perfused areas were determined by invasive coronary angiography. We attempted to select a region of interest of 100 mm^2 in the myocardium that excluded the vessels and perivascular fat. The image noise was defined as the standard deviation (SD) of the attenuation of the normal myocardium. The contrast and contrast-to-noise ratio (CNR) were calculated with the following formula:

$$Contrast = HU_{normal} - HU_{hypo}$$
$$CNR = (HU_{normal} - HU_{hypo})/SD$$

We defined the optimized energy level as that which results in images with the highest CNR. We also measured the iodine concentration and effective Z in the normal and hypo-perfused areas.

Quantitative image analysis

The image quality obtained with the different sequences was evaluated by qualitative image analysis with a PACS viewer (View R, version 1.09.15, Yokogawa Electronic, Tokyo, Japan). Two board-certified radiologists with 20 and 13 years of experience with cardiac CT, respectively, independently graded the image contrast, noise, artifacts, sharpness, and overall image quality.

The CT datasets were randomized, and the readers were blinded to the acquisition parameters. Using a subjective four-point scale, they independently graded image contrast and overall quality (1 = unacceptable, 2 = acceptable, 3 = good, or 4 = excellent). Image noise and artifacts were similarly recorded as grade 1 (present and unacceptable), 2 (present and interfering with the depiction of adjacent structures), 3 (present without interfering with the depiction of adjacent structures), or 4 (no noise or artifacts). Image sharpness was determined by evaluating the aortic wall sharpness as grade 1 (blurry), 2 (poorer than average), 3 (better than average), and 4 (sharp). Any disagreement between the readers was settled by consensus.

Statistical analysis

We performed statistical analyses with the programing software Python (version 3.6.3). The Kolmogorov-Smirnov test was performed to determine the normality of the distributions. All numerical values were expressed as mean ± SD. For quantitative image analysis, we performed the paired t-test to compare the best CNR VMIs and conventional CT images and to compare the iodine concentration and the effective Z in the normal and hypo-perfused areas. For qualitative image analysis, we performed the Wilcoxon Signed Ranks test to compare the best CNR VMIs and conventional CT images. Furthermore, the degree of agreement between two observers regarding the visual evaluation results was measured using kappa

statistics: poor (<0.20), fair (0.21–0.40), moderate (0.41–0.60), substantial (0.61–0.80), and near-perfect (0.81–1.00). Values of $p < 0.05$ were considered statistically significant.

Results

Quantitative image analysis

Figure 1 shows the CT number, image noise, contrast, and CNR between the normal and hypo-perfused myocardium. As the X-ray energy decreased, venous attenuation, contrast, and CNR gradually increased. The 40 keV image offered the best CNR, and thus 40 keV images were selected as the optimized energy VMIs.

Figure 2 shows the qualitative analysis regarding the optimized energy VMIs (40 keV images) and 120 kVp images. There was no significant difference in image noise between the 120 kVp images (12.6 ± 4.8 HU) and 40 keV images (16.6 ± 13.0 HU) ($p = 0.07$). The contrast (120 kVp: 41.5 ± 20.4 HU vs 40 keV: 1113.4 ± 49.0 HU) and the CNR (120 kVp: 3.6 ± 2.0 vs 40 keV: 9.1 ± 6.7) between the normal and hypo-perfused myocardium were significantly higher in 40 keV images than those in 120 kVp images ($p < 0.01$).

Figure 3 shows the iodine concentration and effective Z in the normal and hypo-perfused areas. The iodine concentration and effective Z were significantly higher in normal myocardium (1.4 ± 0.6 mgI/mL and 8.1 ± 0.2, respectively) than those in hypo-perfused myocardium (0.3 ± 0.3 mgI/mL and 7.4 ± 0.4, respectively) ($p < 0.01$).

Quantitative image analysis

Table 2 summarizes the qualitative analysis. The 40 keV images offered significantly higher scores for the image contrast, noise, artifacts, and overall quality ($p < 0.01$). Conversely, there were no significant differences in the sharpness between the 120 kVp and 40 keV images ($p = 0.83$). Inter-observer agreements regarding the image contrast, noise, artifacts, sharpness, and overall quality were moderate (kappa = 0.71, 0.69, 0.70, 0.65, and 0.65, respectively). Representative cases are shown in Figure 4 and 5.

Discussion

Our study suggests that the best CNR VMIs between the normal and hypo-perfused myocardium are obtained with 40 keV images. The image noise of 40 keV images was slightly (but not significantly) higher than that of conventional CT images. Conversely, the contrast and CNR of 40 keV images were significantly higher than those of conventional CT images.

To date, some studies have evaluated CT myocardial perfusion in potential ACS patients [16–19]. Using a 16-MDCT protocol for 69 patients presenting with acute chest pain, Lessick et al. [16] demonstrated that CT-MPI hypo-perfusion had a sensitivity of 67% and a specificity of 95% for diagnosing myocardial

ischemia or infarction. However, most studies acquired myocardial perfusion images using continuous shooting scan that requires additional radiation doses and injections of contrast material. Nagao et al. reported that there was no significant difference in diastolic perfusion between ischemic and nonischemic segments in a conventional CT scanning [19].

In this study, the image noise of VMIs at all energy levels was not significantly higher than that of conventional CT images, and the image contrast and CNR between the normal- and hypo-perfused myocardium were highest with 40 keV. The DL-DECT system simultaneously collects low- and high-energy data in the two detector layers at the exact same anatomical location. Therefore, the VMI reconstruction technique can suppress beam-hardening artifacts and anti-correlated noise in photoelectric and Compton scatter images. In this study, the artifact score at 40 keV was lower in VMIs than that in conventional CT images; however, this difference was not statistically significant. Model-based IR techniques equipped with DL-DECT can achieve further noise reduction [20]. In our study, the IR technique decreased the image noise of VMIs compared with that of conventional CT images.

In addition, we found that the iodine density and effective Z in the ACS regions were significantly lower than those in the normal regions. Although the accuracy of this technique will need to be compared with other techniques, such as myocardial scintigraphy and CT perfusion, we believe that this technique has the potential to quantitatively assess hypo-perfusion in ACS.

Our study has some limitations. First, the study population was small, and our results might not be generalizable. Second, we did not perform diagnostic performance analysis of culprit vessels because of the limited number of patients with multi-vessel stenoses.

In conclusion, spectral imaging with dual-layer spectral detector CT is a feasible technique to detect hypo-perfused areas of acute ischemic syndrome.

Declarations

Funding: Not applicable.

Conflicts of interest/Competing interests: The authors declare no conflicts of interest associated with this manuscript.

Availability of data and material: Not applicable.

Code availability: Not applicable.

Authors' contributions:

Ethics approval / Consent to participate / Consent for publication: This retrospective study received institutional review board approval; the requirement for written informed consent was waived.

References

1. Shah PK, Forrester JS (1991) Pathophysiology of acute coronary syndromes. Am J Cardiol 68:16C-23C. https://doi.org/10.1016/0002-9149(91)90219-b
2. Cimmino G, Conte S, Morello A et al (2012) The complex puzzle underlying the pathophysiology of acute coronary syndromes: from molecular basis to clinical manifestations. Expert Rev Cardiovasc Ther 10:1533–1543. https://doi.org/10.1586/erc.12.157
3. Arbab-Zadeh A, Miller JM, Rochitte CE et al (2012) Diagnostic accuracy of computed tomography coronary angiography according to pre-test probability of coronary artery disease and severity of coronary arterial calcification. The CORE-64 (Coronary Artery Evaluation Using 64-Row Multidetector Computed Tomography Angiography) International Multicenter Study. J Am Coll Cardiol 59:379–387. https://doi.org/10.1016/j.jacc.2011.06.079
4. Takakuwa KM, Halpern EJ (2008) Evaluation of a “triple rule-out” coronary CT angiography protocol: use of 64-Section CT in low-to-moderate risk emergency department patients suspected of having acute coronary syndrome. Radiology 248:438–446. https://doi.org/10.1148/radiol.2482072169
5. Giroud D, Li JM, Urban P et al (1992) Relation of the site of acute myocardial infarction to the most severe coronary arterial stenosis at prior angiography. Am J Cardiol 69:729–732. https://doi.org/10.1016/0002-9149(92)90495-k
6. Little WC, Constantinescu M, Applegate RJ et al (1988) Can coronary angiography predict the site of a subsequent myocardial infarction in patients with mild-to-moderate coronary artery disease? Circulation 78:1157–1166. https://doi.org/10.1161/01.CIR.78.5.1157
7. Branch KR, Busey J, Mitsumori LM et al (2013) Diagnostic Performance of Resting CT Myocardial Perfusion in Patients With Possible Acute Coronary Syndrome. Am J Roentgenol 200:W450–W457. https://doi.org/10.2214/AJR.12.8934
8. Goodsitt MM, Christodoulou EG, Larson SC (2011) Accuracies of the synthesized monochromatic CT numbers and effective atomic numbers obtained with a rapid kVp switching dual energy CT scanner. Med Phys 38:2222–2232. https://doi.org/10.1118/1.3567509
9. Alvarez RE, Macovski A (1976) Energy-selective reconstructions in X-ray computerized tomography. Phys Med Biol 21:733–744. https://doi.org/10.1088/0031-9155/21/5/002
10. Matsumoto K, Jinzaki M, Tanami Y et al (2011) Virtual monochromatic spectral imaging with fast kilovoltage switching: improved image quality as compared with that obtained with conventional 120-kVp CT. Radiology 259:257–262. https://doi.org/10.1148/radiol.11100978
11. Hickethier T, Baeßler B, Kroeger JR et al (2017) Monoenergetic reconstructions for imaging of coronary artery stents using spectral detector CT: In-vitro experience and comparison to conventional images. J Cardiovasc Comput Tomogr 11:33–39. https://doi.org/10.1016/j.jcct.2016.12.005
12. Nagayama Y, Tanoue S, Inoue T et al (2020) Dual-layer spectral CT improves image quality of multiphasic pancreas CT in patients with pancreatic ductal adenocarcinoma. Eur Radiol 30:394–403. https://doi.org/10.1007/s00330-019-06337-y

13. Nagayama Y, Inoue T, Oda S et al (2020) Adrenal Adenomas versus Metastases: Diagnostic Performance of Dual-Energy Spectral CT Virtual Noncontrast Imaging and Iodine Maps. Radiology 296:324–332. https://doi.org/10.1148/radiol.2020192227
14. Oda S, Nakaura T, Utsunomiya D et al (2018) Late iodine enhancement and myocardial extracellular volume quantification in cardiac amyloidosis by using dual-energy cardiac computed tomography performed on a dual-layer spectral detector scanner. Amyloid Int J Exp Clin Investig Off J Int Soc Amyloidosis 25:137–138. https://doi.org/10.1080/13506129.2018.1424625
15. Doherty JU, Kort S, Mehran R et al (2019) ACC/AATS/AHA/ASE/ASNC/HRS/SCAI/SCCT/SCMR/STS 2019 Appropriate Use Criteria for Multimodality Imaging in the Assessment of Cardiac Structure and Function in Nonvalvular Heart Disease: A Report of the American College of Cardiology Appropriate Use Criteria Task Force, American Association for Thoracic Surgery, American Heart Association, American Society of Echocardiography, American Society of Nuclear Cardiology, Heart Rhythm Society, Society for Cardiovascular Angiography and Interventions, Society of Cardiovascular Computed Tomography, Society for Cardiovascular Magnetic Resonance, and the Society of Thoracic Surgeons. J Am Coll Cardiol 73:488–516. https://doi.org/10.1016/j.jacc.2018.10.038
16. Lessick J, Ghersin E, Dragu R et al (2007) Diagnostic accuracy of myocardial hypoenhancement on multidetector computed tomography in identifying myocardial infarction in patients admitted with acute chest pain syndrome. J Comput Assist Tomogr 31:780–788. https://doi.org/10.1097/rct.0b013e318033d6fc
17. Bezerra HG, Loureiro R, Irlbeck T et al (2011) Incremental value of myocardial perfusion over regional left ventricular function and coronary stenosis by cardiac CT for the detection of acute coronary syndromes in high-risk patients: a subgroup analysis of the ROMICAT trial. J Cardiovasc Comput Tomogr 5:382–391. https://doi.org/10.1016/j.jcct.2011.10.004
18. Nagao M, Matsuoka H, Kawakami H et al (2009) Myocardial ischemia in acute coronary syndrome: assessment using 64-MDCT. AJR Am J Roentgenol 193:1097–1106. https://doi.org/10.2214/AJR.08.1965
19. Nagao M, Matsuoka H, Kawakami H et al (2008) Quantification of myocardial perfusion by contrast-enhanced 64-MDCT: characterization of ischemic myocardium. AJR Am J Roentgenol 191:19–25. https://doi.org/10.2214/AJR.07.2929
20. Chang W, Lee JM, Lee K et al (2013) Assessment of a model-based, iterative reconstruction algorithm (MBIR) regarding image quality and dose reduction in liver computed tomography. Invest Radiol 48:598–606. https://doi.org/10.1097/RLI.0b013e3182899104

Tables

Table 1 Scanning parameters and contrast medium infusion protocols for each group

Tube voltage (kVp)	120
Tube current (effective mAs)	Auto mA
Helical Pitch	0.14
Detector collimation (mm)	64×0.625
Rotation time (s)	0.27
Iodine dose (mgI/kg)	240
Bolus tracking trigger (HU)	110
Scan delay (s)	6
Injection duration (s)	13
Image reconstruction	VMI: Spectral level 3, 40–200 keV (at 5 keV intervals)
	Conventional: iDose 3, 120 kVp
Slice thickness (mm)	1

Table 2 Quantitative Analysis

	40 keV	120 kVp	P value
Image contrast	3.78 ± 0.33	2.39 ± 0.66	< 0.001
Image noise	3.88 ± 0.33	3.48 ± 0.51	< 0.001
Artifact	3.33 ± 0.54	3.63 ± 0.49	< 0.001
Sharpness	3.45 ± 0.56	3.42 ± 0.50	0.83
Overall image quality	3.79 ± 0.41	2.85 ± 0.67	< 0.001

*Data are shown as the mean ± standard deviation.

Figures

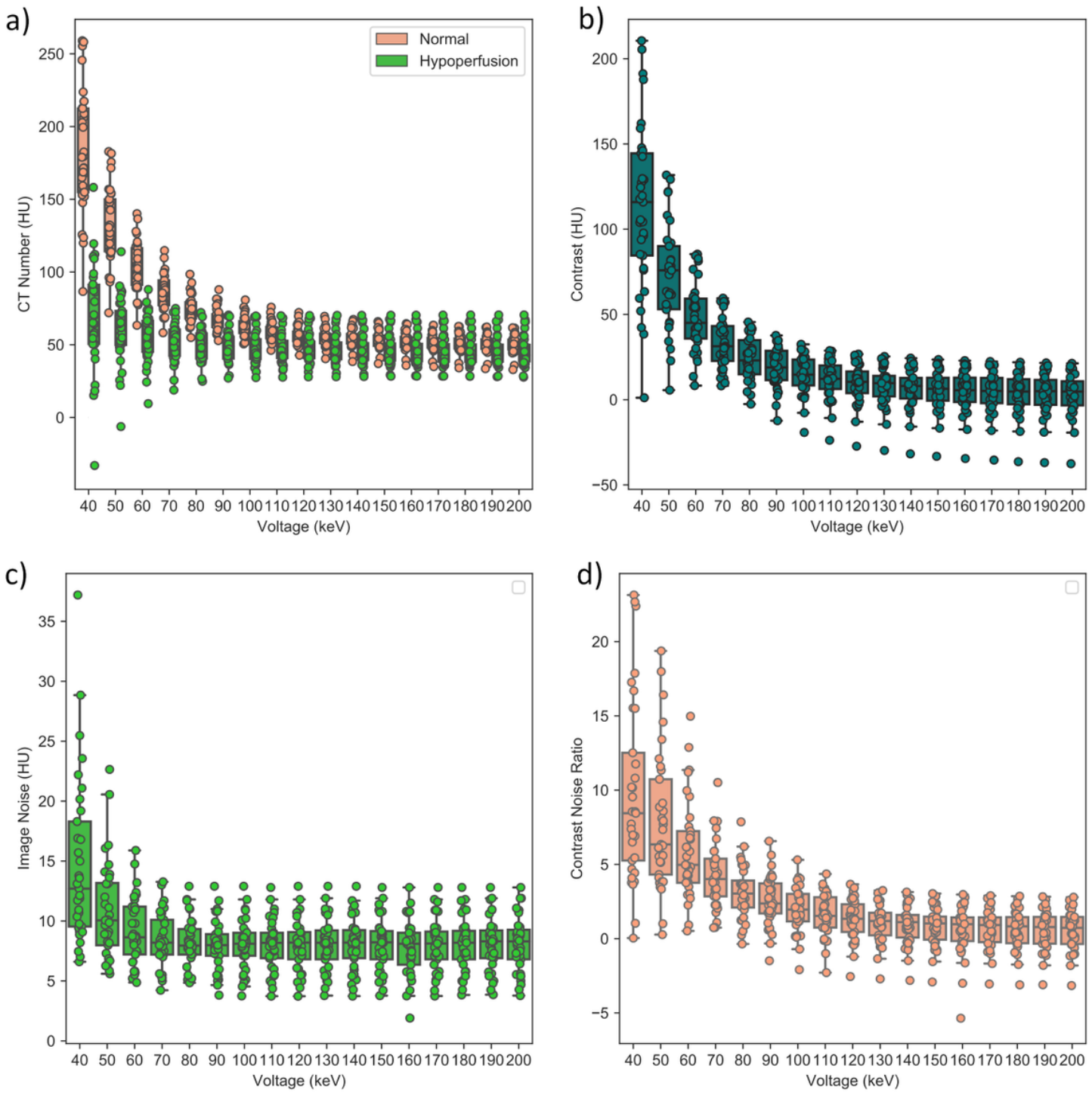

Figure 1

Quantitative image analysis The computed tomography number (a) of the normal myocardium gradually increases with decreasing energy of virtual monochromatic images (VMIs), whereas the difference in hypo-perfused myocardium is not so large. The increase in contrast (b) of low-energy VMIs is greater than the increase in noise (c). The contrast-to-noise ratio (d) is greatest at 40 keV.

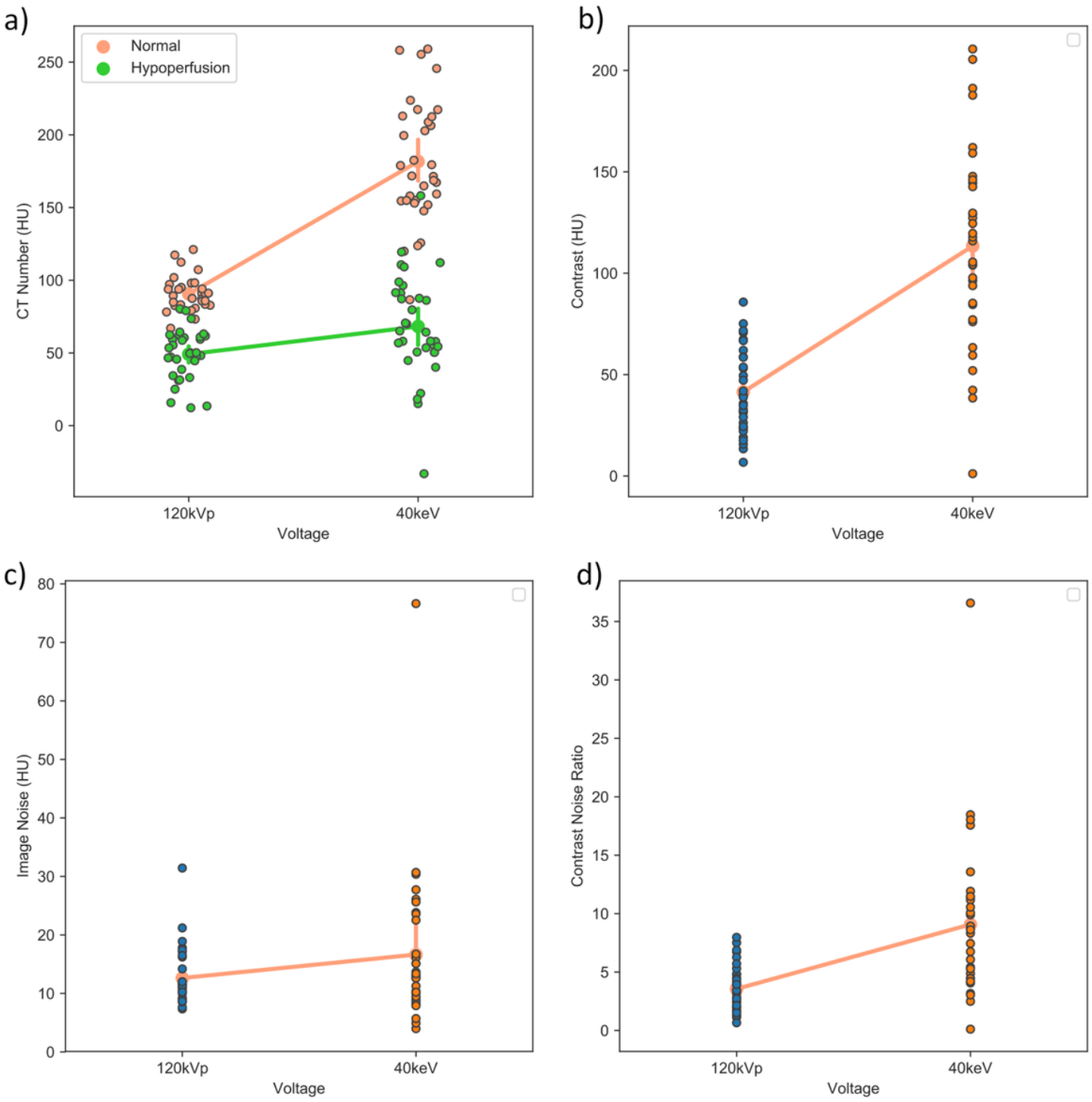

Figure 2

Quantitative image analysis The computed tomography numbers (a) of 40 keV images are significantly higher than those of 120 kVp images of the normal myocardium, whereas the increase is not so notable for hypo-perfused myocardium. The image contrast (b) is significantly higher in 40 keV images than that in 120 kVp images. The image noise (c) does not significantly differ between the two protocols. The contrast-to-noise ratio (d) is significantly higher in 40 keV images than that in 120 kVp images.

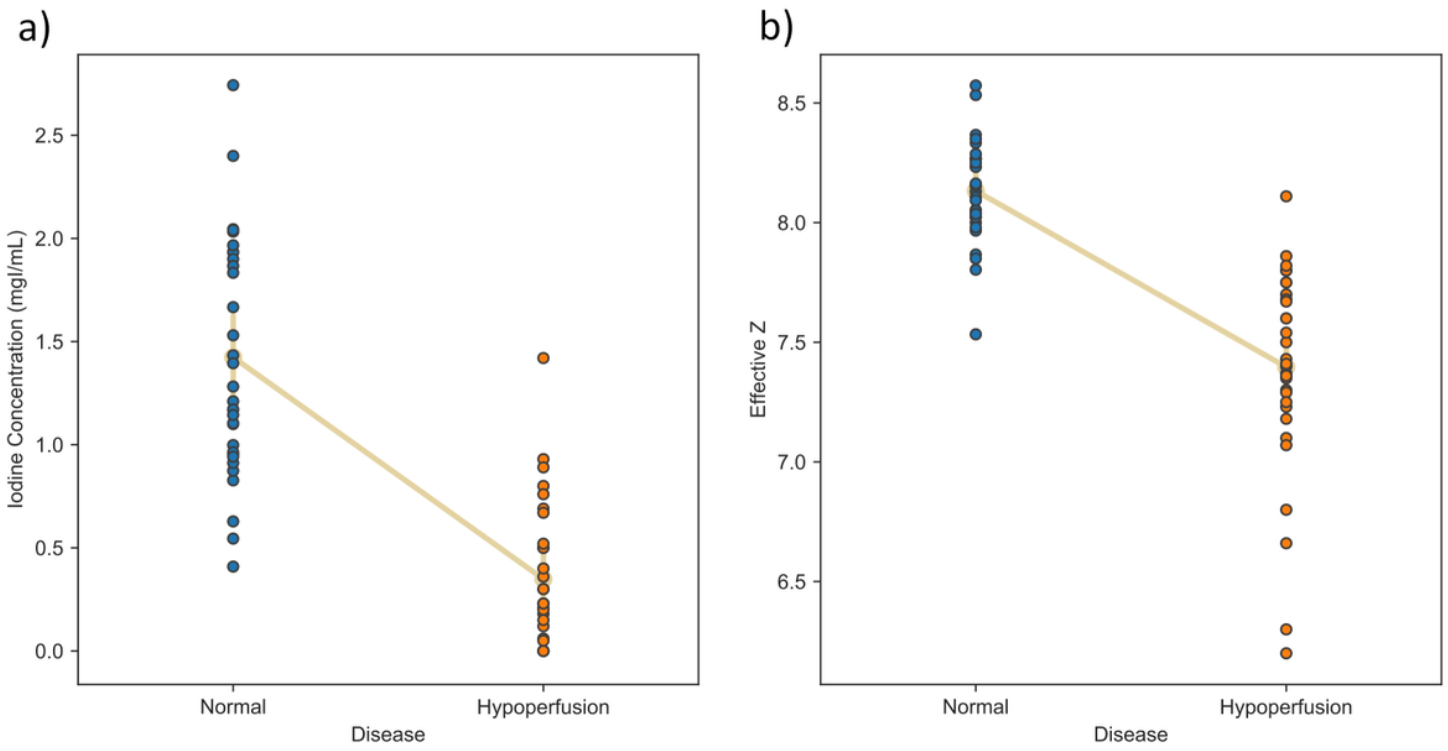

Figure 3

Quantitative image analysis The iodine concentration (a) and the effective atomic number (Z) (b) are significantly higher in 40 keV images of the normal myocardium than those of the hypo-perfused myocardium.

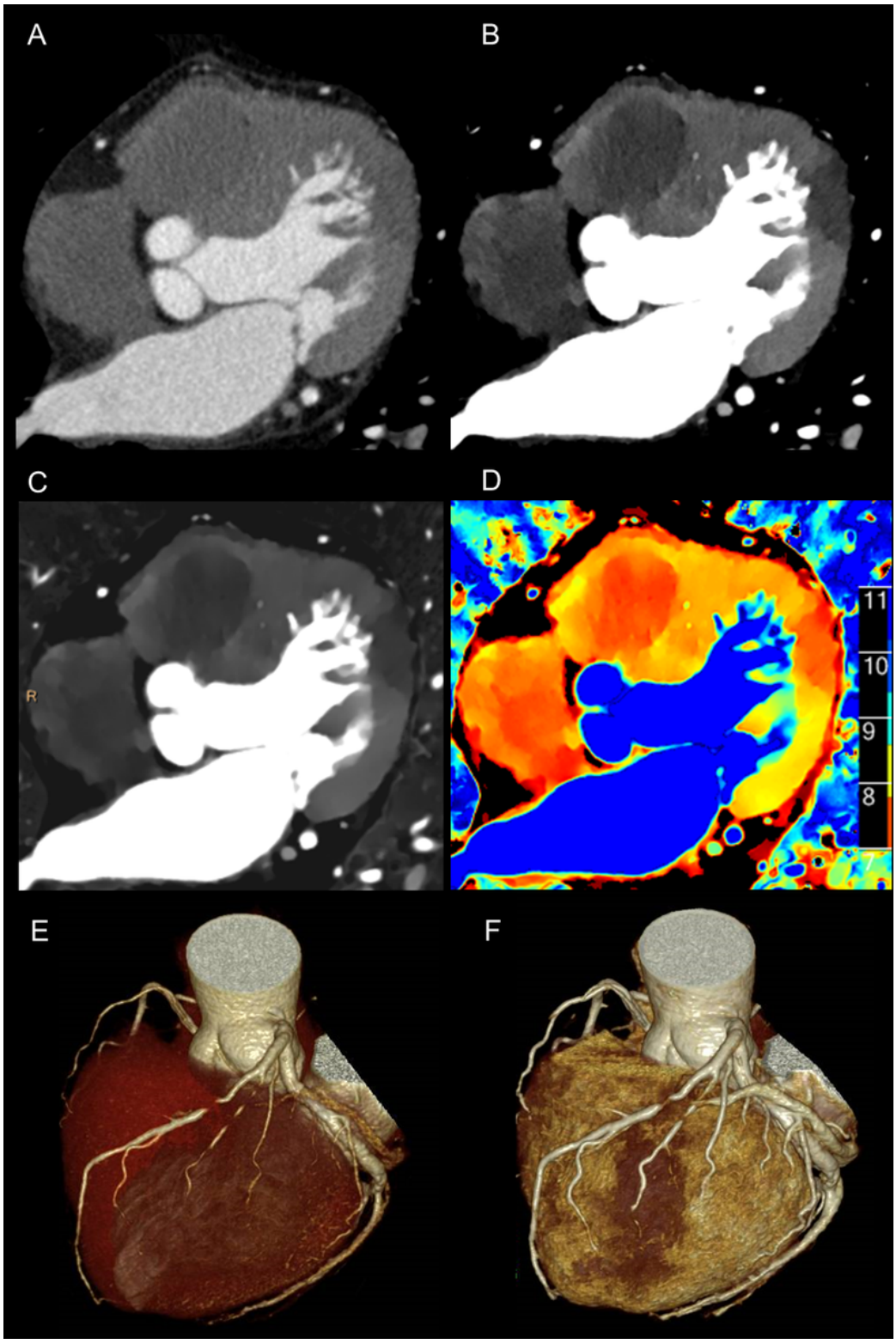

Figure 4

Case 1 A 75-year-old obese man with no prior cardiac history presented with chest pain. Coronary artery evaluation showed severe stenosis in LAD and D2. However, it was not possible to determine the culprit lesion. We performed a myocardial perfusion evaluation. Compared with 120 kVp (A), the 40 keV image (B) clearly depicts the hypo-perfusion area in the D2 segment. The iodine density map (C) and effective Z map (D) clearly depict the iodine defect in the D2 segment. These results suggest that the culprit vessel is

D2. Although invisible at 120 kVp (E), an abnormal area is visible in the VR image at 40keV (F), indicating that the blood vessel in which the perfusion abnormality is occurring is D2.

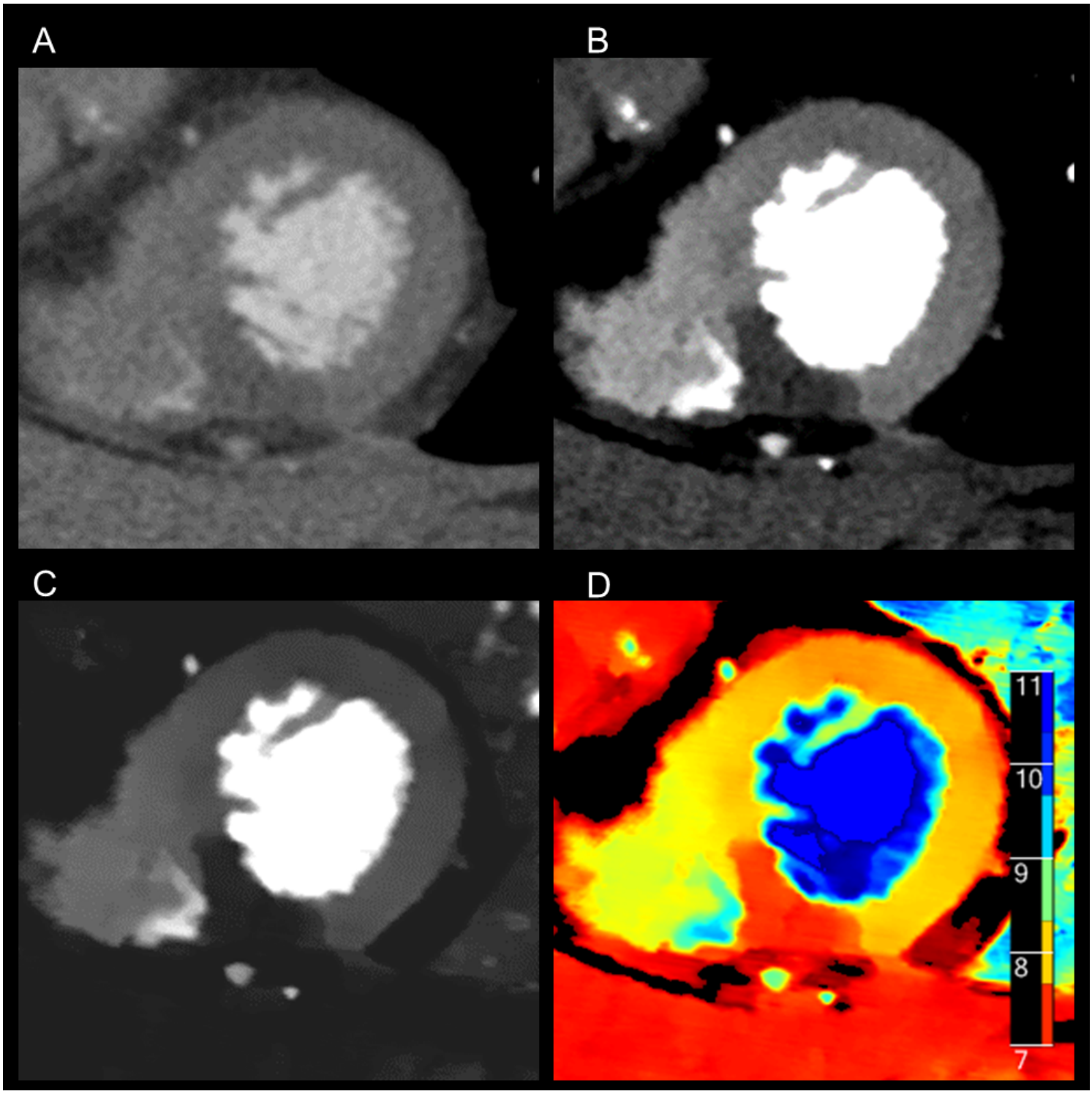

Figure 5

Case 2 A 70-year-old man was admitted to our hospital due to persistent chest pain. Cardiac computed tomography was performed to analyze symptoms; however, no obvious significant stenosis was noted. Nevertheless, perfusion evaluation revealed a hypo-perfused area of the lower apex wall. Additionally, compared to 120 kVp (A), the 40 keV (B), iodine map (C), and effective Z map (D) exhibited clear contrast.